PERGAMON

International Journal of Heat and Mass Transfer 42 (1999) 4535–4548

International Journal of HEAT and MASS TRANSFER

www.elsevier.com/locate/ijhmt

# Modelling of scattering and absorption coefficients for a polydispersion

Miguel Caldas, Viriato Semião*

*Mechanical Engineering Department, Instituto Superior Técnico, Technical University of Lisbon, Av Rovisco Pais, 1096 Lisbon Codex, Portugal*

Received 26 May 1998; received in revised form 8 March 1999

**Abstract**

An adequate treatment of the thermal radiation heat transfer mechanism is essential to a mathematical model of the combustion process or to design a combustion device. Predictive tools using flux models, such as the discrete transfer method, the discrete ordinates method and the spherical harmonics method, that solve the radiative heat transfer equation, require as input the values of the absorption and scattering coefficients of the participating media. Such coefficients must be evaluated in an expedite fashion since computational fluid dynamics and radiative flux models are extremely time demanding by themselves. In this work, a curve fitting approach to the Mie theory is used to evaluate the above-mentioned coefficients for intermediate and large particles, ensuring a compromise between accuracy and computational economy. The same coefficients for small particles are calculated using power series to represent the Mie coefficients accurately and economically. Predictions with the present models were performed for soot, carbon particles and fly ash and are presented herein. The results have proved that the models proposed in this work are computationally much faster than the prohibitive Mie theory calculations: reductions in computing times as high as three-hundred fold. Additionally, the referred models allow for the achievement of very accurate results: a relative error between approximated values and the corresponding Mie exact solution almost always below 5%. 

## 1. Introduction

Radiation is undoubtedly the dominant heat transfer mechanism within the vast majority of industrial combustion systems. The flow and the temperature fields, together with the species concentrations inside combustors, are most influenced by the rate of radiant energy exchanged between the flame and the enclosing walls. Hence, an accurate prediction of the heat transferred by radiation is a key issue in the design and optimisation of the operating conditions of industrial combustion chambers. For the achievement of such accurate predictions the values of the absorption and scattering coefficients of the participating media play a determinant role.

In addition to radiation, the combustor performance is characterised by a two-phase (coal and oil fired combustors) or by a single-phase (gas fired combustors) turbulent combusting flow. If radiation is a determinant heat transfer mechanism, requiring therefore its modelling, the choice of the model has to be effected accordingly to the fluid flow modelling approach.

Many radiation models have been developed for emitting, absorbing and scattering media [1], most of them being based on the solution of the radiative heat

* Corresponding author. Tel.: +351-1-841-7378; fax: +351-1-847-5545.

*E-mail address:* viriato@navier.ist.utl.pt (V. Semião)

0017-9310/99/$ - see front matter 
PII: S0017-9310(99)00106-4

**Nomenclature**

*Symbols*

| | |
|---|---|
| $A_i$ | $i$th weighing factor for Gauss–Laguerre integration |
| $C_i$(m) | curve fitting coefficients ($i$ = 1, 7) for Eqs. (11a) and (11b) |
| $D$ | diameter [m] |
| $D_{20}^2$ | mean quadratic diameter [m$^2$] |
| $k$ | extinction/scattering coefficient [m$^{-1}$] |
| $L$ | asymptotic limit of $Q$ when $x \to \infty$ |
| $L_n^\alpha$ | Laguerre polynomial of order n |
| $m$ | complex refractive index |
| $N(D)$ | disperse phase size distribution [m$^{-1}$] |
| $N_0$ | number of particles per unit volume [m$^{-3}$] |
| $p$ | shape parameter of the size distribution |
| $q$ | shape parameter of the size distribution |
| $Q$ | extinction/scattering efficiency factor |
| $x$ | size parameter |
| $z_i$ | $i$th zero of Laguerre polynomial |
| $\epsilon$ | characteristic value of $x$ for curve fitting |

*Subscripts*

| | |
|---|---|
| c | characteristic value |
| e | extinction |
| s | scattering |

transfer equation (RHTE). Some of those models are not recommended for coupling with combusting fluid flow modelling, despite their recognised accuracy. These are the cases of the zonal method [2] and the Monte Carlo method [3], that require much too long computing times and make recourse to numerical techniques very different from those used in fluid flow predictions.

All the other commonly used models make recourse to the flux method that discretises the space into a finite number of solid angles and assume the heat flux as constant within each solid angle in order to eliminate the directional dependence of the RHTE. The use of the third order approximation (P3) of the spherical harmonics method (Pn models, n being the method approximation order) has produced accurate results for two-dimensional geometries, both for Cartesian co-ordinates [4] and cylindrical co-ordinates—axially symmetric geometries [5], as well as for three-dimensional geometries in Cartesian co-ordinates [6]. However, the method has proved to be mathematically involved to obtain accurate predictions.

Two more attractive algorithms for coupling with ordinary fluid flow predictive tools, the discrete ordinates method [7] and the discrete transfer method [8], have produced very accurate results in solving the RHTE [8–14].

The three previous methods require as input the gas and the solid particles absorption coefficients, the particles scattering coefficient and, for anisotropic scattering, the phase function of the participating media. Furthermore, it was shown by [5] that the radiative heat flux distribution is rather sensitive to the variation of the absorption and scattering coefficients of the participating media. Hence, the accuracy in calculating the previous coefficients will determine the precision of the predicted radiation heat fluxes.

The values for the above-mentioned coefficients could be evaluated by the use of Mie theory [15]. However, even making recourse to efficient algorithms and high-speed computers, its use in numerical predictive tools is unimaginable, due to its mathematical involvement and prohibitive computational time requirements. An accurate and economic modelling is, therefore, mandatory.

Even for gaseous flames, most of the current work on the modelling of industrial combustion chambers using computational fluid dynamics (CFD) codes makes recourse to polynomial approximations to predict the total radiative properties of the absorbing media. The reason for this stems from the necessity to minimise the time required for the computation of those properties. Those models reached an unpaired success in the numerical modelling of industrial flames due both to their simplicity and reasonable accuracy to simulate the properties of gaseous combustion products at common temperatures and pressures operating ranges of real life furnaces. However, increasing interest shown by industrials together with the need to comply with different operating conditions and modelling (e.g. gas turbines or kinetically controlled combustion) require more general models to predict the radiative properties of gaseous absorbing media. The exponential wide band model appears to be a promising approach. However, it is recognised that even this model is much too time demanding for inclusion in this kind of simulation, the result being the rise of a wide variety of simplified approaches that resort to curve fitting and other empirical methods [16–20]. Should the combustion chamber be fired with oil or coal, the necessity for the calculation of the solid

phase scattering/extinction properties with recourse to extremely expeditious and simultaneously accurate models will be even more mandatory.

This concern with the computational time requirements is more than legitimate. Indeed, if radiation calculations are to be coupled with the finite volume approach for CFD computations the extinction/scattering coefficients will vary for each iteration, which causes a variation of the gas composition, particles type and size distribution at each control volume covering the combustion chamber physical domain. Additionally, the control volumes temperatures also changes within the iterative procedure causing a corresponding change in the dominating radiative wavelength, in turn responsible for the size parameter value modification. This will induce a further deviation of the extinction/scattering coefficients values, resulting therefore in the need for evaluation of the discussed coefficients for each control volume and CFD iteration. Since CFD/combustion calculations and radiative transfer equations modelling are by themselves very computer time demanding, there is an absolute need not to overload the whole simulation with another highly time demanding calculation. Those facts explain the necessity of an extremely efficient algorithm for the calculation of the extinction and scattering coefficients.

The ultimate objective of the present research effort is the development of an accurate and economic procedure to evaluate radiative properties of polydispersions, commonly present in combustion chambers, to feed the RHTE that, in turn, must be coupled with CFD calculations.

In the present work, models to accurately and economically approximate the results of the Mie theory (used herein as a reference solution) for the evaluation of the absorption and scattering coefficients for different types of polydisperse solid phase, such as soot, carbon particles and fly ash, are proposed.

Some authors consider the Mie theory limited for the radiation heat transfer calculations in practical applications, such as particle-laden boilers, since it describes the far-field scattering of plane waves interacting with isolated, homogeneous and spherical particles. This means that particles are assumed to be independent scatterers. Despite this arguing, Mie theory has proved to be applicable in practical systems with volume fractions below 0.006 or with a clearance-to-wavelength ratio above 0.5, as conservatively stated by [21]. Indeed, [22] presented a less conservative upper limit value of 0.1 for the volume fraction. In most particulate combustion systems the volume fraction is below $10^{-3}$ and, therefore, Mie theory still applies. This has been widely supported in the literature [1,23]. As far as the assumption of spherical particles is concerned, the work of [21] has stated that even for non-spherical particles their random orientation in a cloud will produce a similar effect to that of a cloud of spherical particles.

In radiating environments the polydisperse solid phase is the only responsible media for the scattering phenomenon, having also a contribution to the radiant energy absorption/emission. The corresponding coefficients depend on the solid phase concentration, on the particles size distribution and on the equivalent coefficients of a single particle.

Asymptotic approximations of the Mie theory, both for large (geometrical optics) and small (Rayleigh theory) particles, exist in the literature [15]. However, particles with an intermediate size lack of a simplified approach for a general complex refractive index. For a value close to unity of that parameter, [23] has tuned an approximation proposed by [15] for the absorption and scattering coefficients, that is valid for particles of intermediate and large sizes.

A different approach to approximate the Mie theory, followed by [24] and [10], is to resort to curve fitting.

In the present work the absorption and scattering coefficients are calculated by a combination of the previous approaches. Indeed, a curve fitting approach is used for intermediate and large particles, but, in opposition to the previous works, the values of the absorption and scattering coefficients are herein fixed by the Mie theory at the origin and by the asymptotic limit at infinity. Additionally, for small particles, the above mentioned coefficients are calculated from power series to represent the Mie coefficients as suggested by [25].

As far as the size distribution of the polydisperse solid phase is concerned, several functions can be found in the literature. A possible distribution to be used for the purpose of the present work is the normalised form of the Nukiyama–Tanasawa function [21,24]. This normalised distribution is completely defined by three parameters: one related to the size of the particles and the remaining two to the distribution shape. For the case of soot and fly ash, the experimental values of [24] and [26] and the theoretical analysis of [24] have determined the two shape parameters of the distributions. For the case of cenospheres, consisting of ash and unburnt carbon formed by the liquid-phase pyrolysis in spray combustion, it is reasonable to assume that the distribution exhibits a shape similar to that of the original liquid spray. The theoretical work of [27] has determined the two shape parameters of spray distributions and [28] used those parameters for spray calculations attaining good agreement with experimental results. The shape parameters for carbon particles and fly ash were empirically set by [24]. In the present study, the shape parameters used to define the size distribution of the different types of polydisperse solid phase were retained from the above mentioned works.

## 2. Analysis and modelling

The monochromatic extinction and scattering coefficients of a polydisperse cloud consisting of spherical particles are given by the following equation:

$$k_{\mathrm{e,\,s}}(N(D), m) = N_0 \frac{\pi}{4} \int_0^\infty D^2 N(D) Q_{\mathrm{e,\,s}}(x, m)\, \mathrm{d}D \tag{1}$$

where $k_{\mathrm{e,s}}$ represents the extinction or scattering coefficient, $Q_{\mathrm{e,s}}$ is the extinction or scattering efficiency factor, $m$ is the complex refractive index, $x$ is the size parameter given by $x = \pi D/\lambda$, $\lambda$ being the wavelength, $N(D)$ is the size distribution and $N_0$ is the total number of particles per unit volume. The absorption coefficient $k_{\mathrm{a}}$ can be easily found from $k_{\mathrm{a}} = k_{\mathrm{e}} - k_{\mathrm{s}}$.

The size distribution $N(D)$ can be adequately represented by a Nukiyama–Tanasawa or modified gamma distribution [21,24]. The following normalised Nukiyama–Tanasawa distribution is always used herein:

$$N(D) = \frac{qC\left(\dfrac{p+1}{q}\right)}{\Gamma\left(\dfrac{p+1}{q}\right)} D^p \exp(-CD^q) \tag{2}$$

where $p$, $q$ and $C$ are distribution parameters and $\Gamma(x)$ is the gamma function.

Defining a characteristic diameter $D_{\mathrm{c}}$ as in Eq. (3), it is possible to rewrite the previous distribution in a more convenient form—Eq. (4).

$$D_{\mathrm{c}} = \left(\frac{1}{C}\right)^{1/q} \tag{3}$$

$$N(D) = \frac{q}{D_{\mathrm{c}} \Gamma\left(\dfrac{p+1}{q}\right)} \left(\frac{D}{D_{\mathrm{c}}}\right)^p \exp[-(D/D_{\mathrm{c}})^q] \tag{4}$$

Substituting Eq. (4) into Eq. (1) and performing an adequate change of the integration variable, the extinction and scattering coefficients become:

$$k_{\mathrm{e,s}} = N_0 \frac{\pi D_{20}^2}{4} \frac{1}{\Gamma\left(\dfrac{p+3}{q}\right)} \int_0^\infty \varphi^{\frac{p+3}{q}-1} \mathrm{e}^{-\varphi} Q_{\mathrm{e,s}}(x_{\mathrm{c}} \varphi^{1/q}, m)\, \mathrm{d}\varphi \tag{5}$$

In Eq. (5) $x_{\mathrm{c}}$ is the size parameter referred to $D_{\mathrm{c}}$ and $D_{20}^2$ is the quadratic mean diameter obtained from the following definition:

$$D_{ij}^{i-j} = \frac{\displaystyle\int_0^\infty D^i N(D)\, \mathrm{d}D}{\displaystyle\int_0^\infty D^{\,j} N(D)\, \mathrm{d}D} = \frac{\Gamma\left(\dfrac{p+1+i}{q}\right)}{\Gamma\left(\dfrac{p+1+j}{q}\right)} D_{\mathrm{c}}^{i-j} \tag{6}$$

In order to permit its numerical integration at lower computational costs, so that the present approach is economically appropriate for radiation predictions, Eq. (5) is modified, resulting in:

$$k_{\mathrm{e,s}} = N_0 \frac{\pi D_{20}^2}{4} \left[ L_{\mathrm{e,s}}(m) + \frac{1}{\Gamma\left(\dfrac{p+3}{q}\right)} \int_0^\infty \varphi^{\frac{p+3}{q}-1} \mathrm{e}^{-\varphi} F_{\mathrm{e,s}}(x_{\mathrm{c}} \varphi^{1/q}, m)\, \mathrm{d}\varphi \right] \tag{7}$$

where $L_{\mathrm{e,s}}(m)$ is the asymptotic limit of the extinction or scattering efficiency factor $Q_{\mathrm{e,s}}(x, m)$ for large values of $x$ that can be found in [15]. The function $F(x, m)$ appearing in Eq. (7) is defined by Eq. (8a) and has the properties represented by Eqs. (8b) and (8c).

$$F_{\mathrm{e,s}}(x, m) = Q_{\mathrm{e,s}}(x, m) - L_{\mathrm{e,s}}(m) \tag{8a}$$

$$F_{\mathrm{e,s}}(0, m) = -L_{\mathrm{e,s}}(m) \tag{8b}$$

$$\lim_{x \to \infty} F_{\mathrm{e,s}}(x, m) = 0 \tag{8c}$$

This function as appearing in Eq. (7) poses fewer mathematical difficulties in integration than $Q_{\mathrm{e,s}}(x, m)$ in Eq. (5). Nevertheless, the integration of Eq. (7) still has to be performed numerically. Its form strongly suggests the use of the following Gauss–Laguerre quadrature formula:

$$\int_0^\infty x^\alpha \mathrm{e}^{-x} f(x)\, \mathrm{d}x = \sum_{i=1}^n A_i f(z_i) \tag{9}$$

In this formula $z_i$ are the zeros of the generalised Laguerre polynomial of order $n$ ($L_n^\alpha(x)$) given by Eq. (10a) and $A_i$ are the weighting factors given by Eq. (10b)—see [29].

$$L_n^\alpha(x) = [x - (\alpha + 2n - 1)] L_{n-1}^\alpha(x) - (n-1)(\alpha + n - 1) L_{n-2}^\alpha(x)$$

$$L_0^\alpha(x) = 1, \quad L_1^\alpha(x) = x - \alpha - 1 \tag{10a}$$

$$A_i = \frac{(n-1)!\Gamma(n+\alpha) z_i}{n(n+\alpha)[L_{n-1}^\alpha(z_i)]^2} \tag{10b}$$

Since the value of $(p+3)/q$ appearing in Eq. (7) is not known beforehand it is necessary to use a quadrature set for $\alpha=0$ and to include the term $\varphi^{(p+3)/q-1}$ in the integrand, which will result in an increase of the number of points required to evaluate the integral with the desired accuracy.

At this point it is necessary to calculate the function $F_{e,s}(x, m)$. This could be done using the Mie theory, however, the computational effort required for these calculations would be prohibitive.

An alternative approach is used in this work and consists of finding a new function depending on $x$, the coefficients of which depend on $m$. Two distinct alternative approximations, each using seven coefficients $C_i(m)$, are described by Eqs. (11a) and (11b) and their accuracy is assessed:

$$F(x,m)\approx\frac{C_1(m)}{1+C_2(m)x^{c_3(m)}}-\frac{L(m)+C_1(m)+C_6(m)x^{C_7(m)}}{1+C_4(m)x^{C_5(m)}} \tag{11a}$$

$$F(x,m)\approx\frac{C_1(m)}{1+C_2(m)x^{C_3(m)}}-\frac{L(m)+C_1(m)}{1+C_4(m)x^{C_5(m)}}\cos\{C_6(m)[(1+C_7(m)x^2)^{1/2}-1]\} \tag{11b}$$

Although Eq. (11b) is more accurate to model near-real refractive indexes, where resonance peaks appear, Eq. (11a) is preferred for numerical modelling, because of its smaller computational effort requirements and better accuracy for refractive indexes with larger imaginary part.

The coefficients appearing in Eqs. (11a) and (11b) can be calculated for each $m$, through a least square regression scheme that fits these equations to Mie theory, and can be stored as a table for later use, in the solution of the RHTE coupled with CFD algorithms.

It must be noticed that in some cases Eqs. (11a) and (11b) become highly inaccurate for small values of $x$. In order to overcome this shortcoming it is necessary to resort to a different approach. For small values of the non-dimensional size parameter and of the refractive index the efficiency factors $Q_{e,s}(x, m)$ can be satisfactorily approximated by a power series retaining a few terms. For example, [25] presented a four-term expansion in the form:

$$Q_e(x,m)=x(E_1(m)+E_2(m)x^2+E_3(m)x^3+E_4(m)x^4) \tag{12a}$$

$$Q_s(x,m)=x^4(S_1(m)+S_2(m)x^2+S_3(m)x^3+S_4(m)x^4) \tag{12b}$$

where $E_i(m)$ and $S_i(m)$ are complex functions that can be found in the work of [25] and are therefore not reproduced here.

These equations can be inserted into Eq. (5) and integrated analytically, yielding:

$$k_e=\frac{N_0\pi D_{20}^2}{4\Gamma\left(\frac{p+3}{q}\right)}x_c\left[E_1(m)\Gamma\left(\frac{p+4}{q}\right)+E_2(m)\Gamma\left(\frac{p+6}{q}\right)x_c^2+E_3(m)\Gamma\left(\frac{p+7}{q}\right)x_c^3+E_4(m)\Gamma\left(\frac{p+8}{q}\right)x_c^4\right] \tag{13a}$$

$$k_s=\frac{N_0\pi D_{20}^2}{4\Gamma\left(\frac{p+3}{q}\right)}x_c^4\left[S_1(m)\Gamma\left(\frac{p+7}{q}\right)+S_2(m)\Gamma\left(\frac{p+9}{q}\right)x_c^2+S_3(m)\Gamma\left(\frac{p+10}{q}\right)x_c^3+S_4(m)\Gamma\left(\frac{p+11}{q}\right)x_c^4\right] \tag{13b}$$

The extent to which Eqs. (13a) and (13b) are accurate is strongly dependent on the value of both the real and imaginary parts of the refractive index $m$. Larger values of $m$ lead to a sooner departure from Mie theory of the values of $k_e$ and $k_s$. It may happen that a range of the non-dimensional size parameter exists where none of the three previously proposed approximations is accurate. In this case, similar expressions to those represented by Eqs. (13a) and (13b) can be used, providing the replacement of the parameters $E_4(m)$ or $S_4(m)$ by $E^*(\epsilon, m)$ or $S^*(\epsilon, m)$—Eqs. (14a) and (14b)—where $\epsilon$ is a value of $x$ that makes Eqs. (11a) and (11b) sufficiently accurate.

$$E^*(\epsilon,m)=\frac{L(m)+F(\epsilon,m)}{\epsilon^5}-\frac{E_1}{\epsilon^4}-\frac{E_2}{\epsilon^2}-\frac{E_3}{\epsilon} \tag{14a}$$

$$S^*(\epsilon,m)=\frac{L(m)+F(\epsilon,m)}{\epsilon^8}-\frac{S_1}{\epsilon^4}-\frac{S_2}{\epsilon^2}-\frac{S_3}{\epsilon} \tag{14b}$$

In summary, the approximate solutions to the Mie theory considered in the present work to evaluate the scattering/extinction coefficients are as follows.

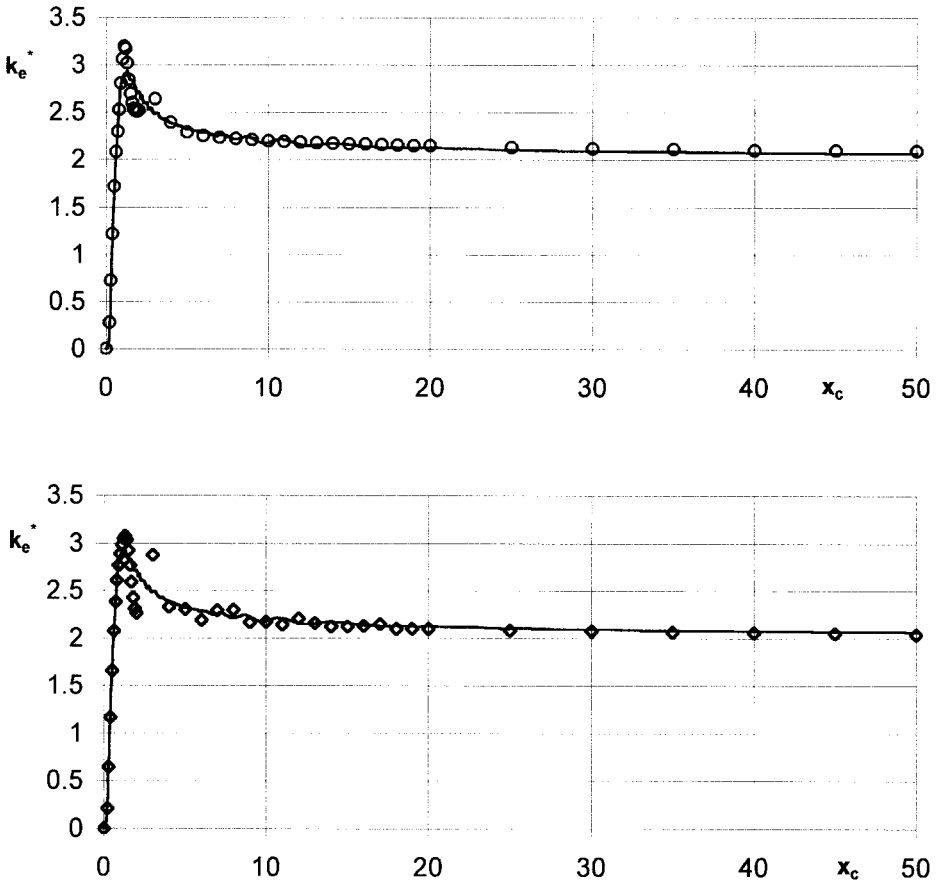


Fig. 1. Comparison of exact and approximate solutions of non-dimensional extinction coefficient for case 1—fly ash ($m = 1.5–0.02i$, $p = 1$, $q = 1$).—exact solution; ○—approximation 1; ◇—approximation 2.

1. Approximation 1—calculated through Eqs. (7) and (11a), the integration being performed using a Gauss–Laguerre quadrature with 5 points, that ensures a compromise between accuracy and economy.
2. Approximation 2—calculated through Eqs. (7) and (11b), the integration being similarly performed.
3. Approximation 3—calculated through Eqs. (13a) for extinction or (13b) for scattering.
4. Approximation 4—calculated through Eqs. (13a) and (14a) for extinction or (13b) and (14b) for scattering, with $\epsilon = 2$ and $F(\epsilon, m)$ calculated through Eq. (11a).

The exact solution is calculated only for comparison purposes and is obtained from the use of Eq. (5), where the efficiency factors are calculated from the Mie theory and the integration is performed using a Gauss–Laguerre quadrature with seventy points, which makes its calculation prohibitively expensive, for inclusion in CFD calculations.

## 3. Case studies, results and discussion

In the present work three different cases are studied in order to validate the proposed models for distinct disperse solid phases (fly ash and carbon particles) and for different shapes of the Nukiyama–Tanasawa particle size distribution. Narrow and broad distributions are obtained by setting different values to the shape characterising parameters $p$ and $q$. In each studied case, both exact and approximate non-dimensional extinction or scattering coefficients, defined as $k^*_{e,s} = 4k_{e,s}/\pi N_0 D^2_{20}$, are plotted against $x_c$, together with the relative error of the approximations.

### *3.1. Case 1: extinction coefficient for fly ash with broad size distribution*

The first case studied in this work (case 1) is characteristic of fly ash. The refractive index used (1.5–0.02 $i$) is that proposed by [10] and corroborated by [21]

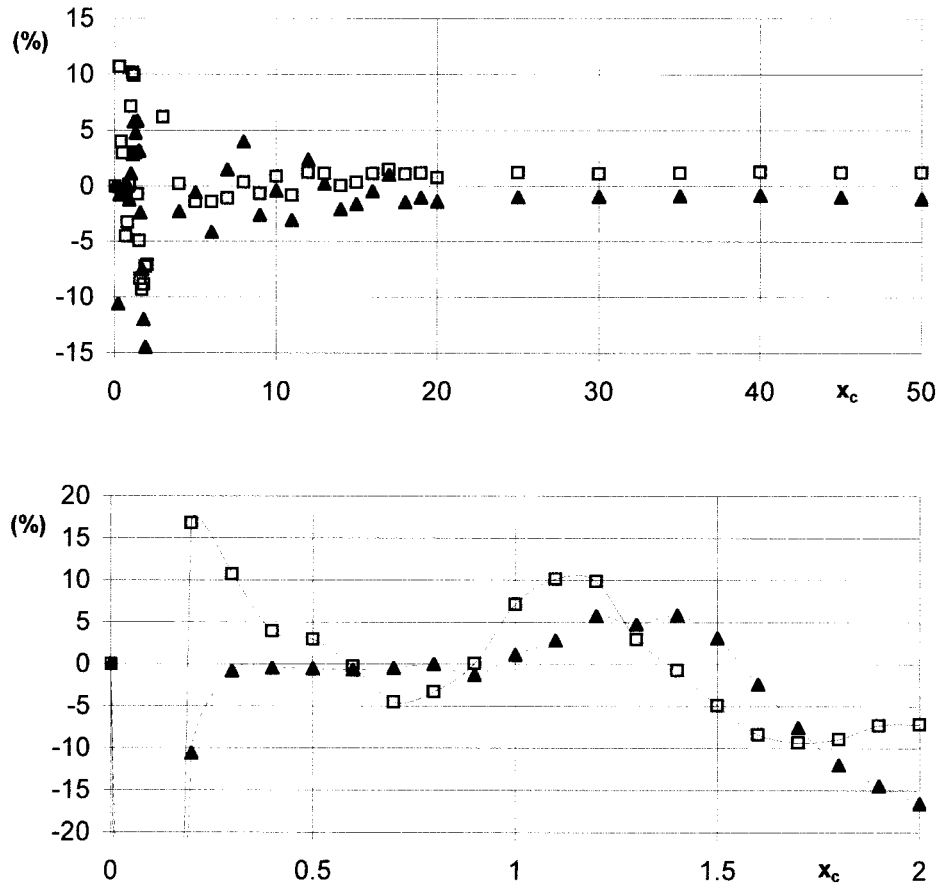


Fig. 2. Error analysis for the comparison of exact and approximate solutions of non-dimensional extinction coefficient for case 1—fly ash ($m = 1.5-0.02i$, $p = 1$, $q = 1$). □, approximation 1; ▲, approximation 2.

and [23] and the distribution shape parameters, $p = 1$ and $q = 1$, are those proposed by [24]. For this case the analysis is focused on the extinction coefficient.

Fig. 1 depicts the values of the non-dimensional extinction factors for this case, both for approximations 1 and 2, compared against the values obtained from the Mie theory, while Fig. 2 shows the error relative to the exact solution of those approximations. As it can be observed from this figure the agreement is very good—within 5% of the relative error—for values of $x_c$ greater than 4.0. For $x_c$ values between 0.25 and 4.0 the agreement is good—not exceeding 15 % of the relative error. On the other hand, for values of $x_c$ between 4.0 and 20.0, the approximated solution containing the cosine function shows poorer agreement. Although Eq. (11b) fits the values obtained from the Mie theory more accurately than Eq. (11a), when the Gauss–Laguerre numerical integration is performed, and because only five points are used, the presence of a cosine function in the integrand leads to a less accurate result. As it was foreseen, for values of $x_c$ below 0.2 approximations 1 and 2 break down.

The computational time required using approximation 1, which is recommended for $x_c \geq 0.25$, is 320 times lower than that requested by the exact solution.

In the range of $x_c$ values below 0.25, approximations 3 and 4 must be used. As it can be seen from Fig. 3, for values of $x_c$ below 0.1, approximation 3 is excellent, despite its departure from the exact solution for greater values. Therefore, for $x_c$ values between 0.12 and 0.25 approximation 4 proved to be the most accurate.

The values of the constants appearing in Eqs. (11a) and (11b) used for this case are presented in Table 1.

### 3.2. Case 2: scattering coefficient for fly ash with narrow size distribution

The second case (case 2) is similar to the first one as far as the type of particles is concerned but the size distribution is modified in order to determine the sensitivity of the results to this parameter and the analysis is focused on the scattering coefficient. In this case the values used for the distribution shape parameters are

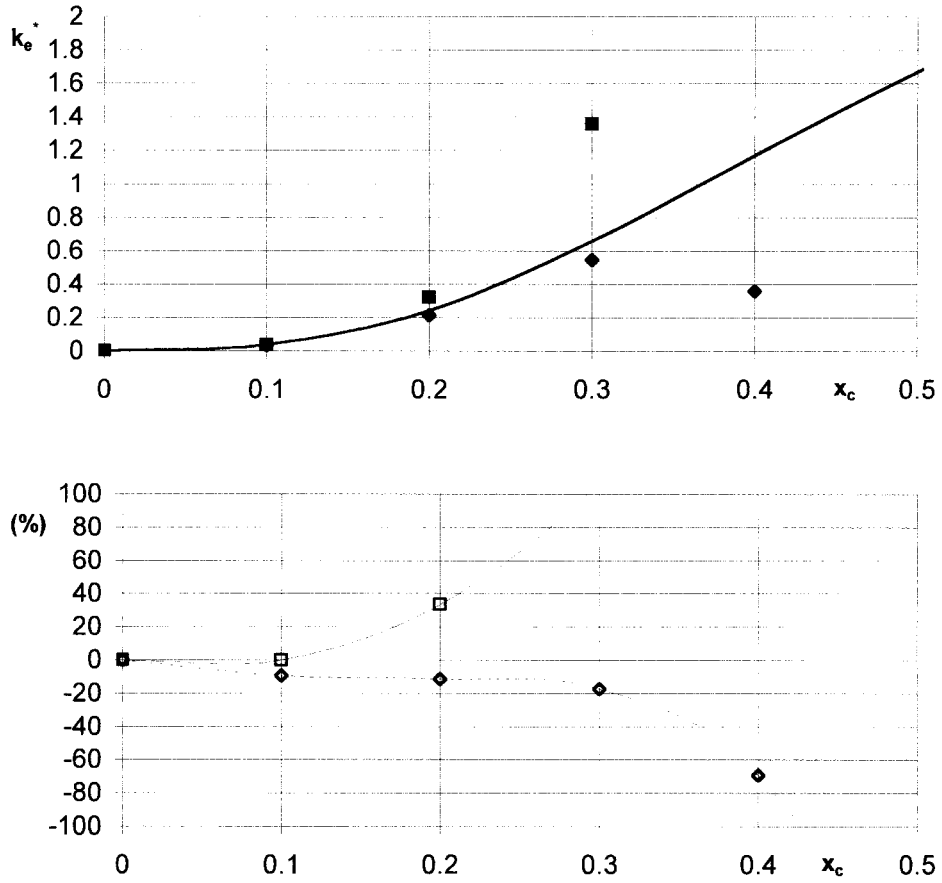


Fig. 3. Comparison and error analysis of exact and approximate solutions of non-dimensional extinction coefficient for case 1—fly ash ($m = 1.5-0.02i$, $p = 1$, $q = 1$). —, exact solution; ■, approximation 3; ◆, approximation 4; □, error of approximation 3; ◇, error of approximation 4.

$p = 4$ and $q = 4$, that correspond to a narrower shape of the distribution.

Fig. 4 shows the predicted values of the non-dimensional scattering factors using approximations 1 and 2 and their comparison against the Mie theory values, while Fig. 5 shows the relative error between those approximations and the exact solution. As for the previous case, it can be observed from Fig. 5 that the agreement in the present case is also very good—within 5.0% of the relative error—for values of $x_c$ greater than 20.0. When compared to case 1 where the asymptotic limit of the extinction efficiency is exact, the present case exhibits a slightly greater relative error due to the fact that the above mentioned limit value for scattering is calculated in an approximated fashion. For $x_c$ values between 1.5 and 20.0 the agreement for both approximations is good—never exceeding 10% of the relative error—although approximation 1 reveals a superior agreement. In this case approximations 1 and 2 break down sooner ($x_c$ values below 1.5) than in the previous case, due to the effect of the disperse solid phase size distribution form, which is narrower ($p = 4$ and $q = 4$).

Approximation 1, that is the one to be used for

Table 1
Curve fitting constants for non-dimensional extinction coefficient ($m = 1.5-0.02i$)

| | $C_1$ | $C_2$ | $C_3$ | $C_4$ | $C_5$ | $C_6$ | $C_7$ |
|---|---|---|---|---|---|---|---|
| Equation (11a) | 1.3560 | 0.7415 | 0.5949 | $1.5\ 10^{-6}$ | 9.0326 | −1.0125 | 1.2559 |
| Equation (11b) | 1.7974 | 0.3108 | 0.9589 | 0.1825 | 1.6850 | 1.6367 | 0.3722 |

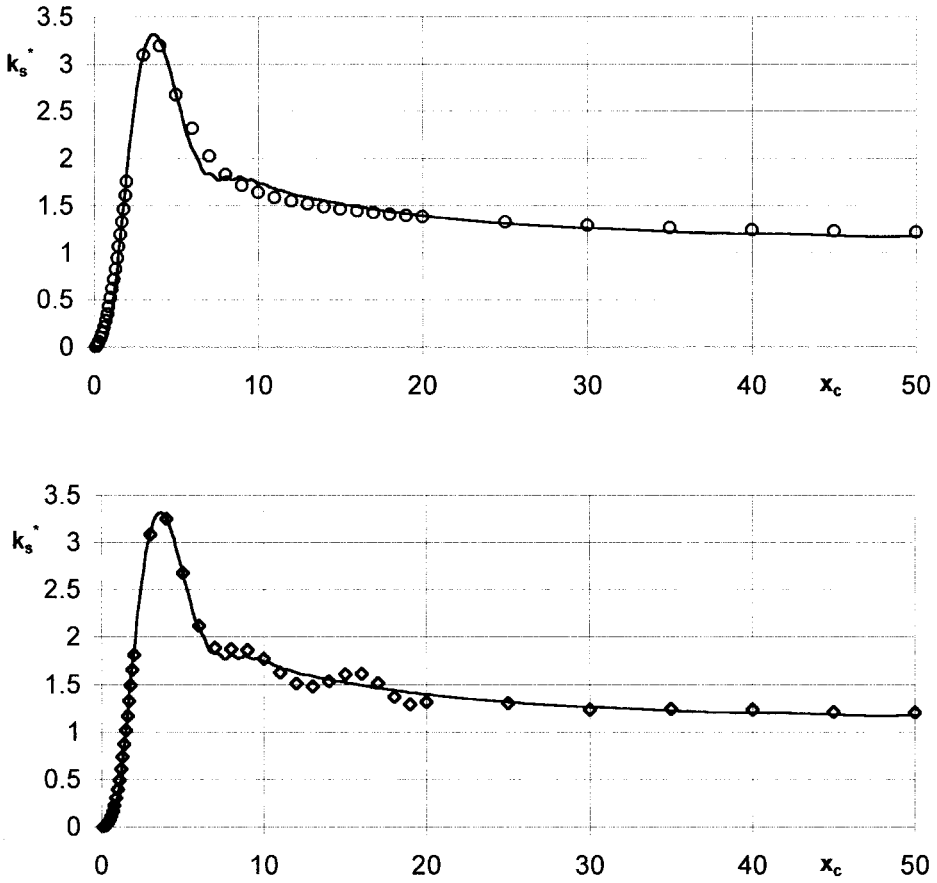


Fig. 4. Comparison of exact and approximate solutions of non-dimensional scattering coefficient for case 2—fly ash ($m = 1.5-0.02i$, $p = 4$, $q = 4$). —, exact solution; ○, approximation 1; ◇, approximation 2.

$x_c \geq 1.5$, requires a computational time 66 times lower than that of the exact solution.

For the range of $x_c$ values below 1.5, approximations 3 and 4 have to be used. Fig. 6 confirms this as for values of $x_c$ below 0.2, approximation 3 is perfect, despite its deviation from the exact solution for greater values. Nevertheless, for values of $x_c$ until 0.7 this approximation is the best one although infirming from an error going up to 28% (see Fig. 6). For $x_c$ values between 0.7 and 1.5 approximation 4 has showed to be the most accurate (relative error below 20%).

It could be expectable a larger relative error for the scattering coefficient of the broader particle size distribution. However, in the studied cases this was not observed. The choice of the two cases out of four presented herein was random, as the differences in the plotted errors of all cases were minimal.

Table 2 displays the values of the constants appearing in Eqs. (11a) and (11b) obtained for this case.

### 3.3. Case 3: extinction coefficient for carbon particles

The last case studied herein (case 3) is characteristic

Table 2
Curve fitting constants for non-dimensional scattering coefficient ($m = 1.5-0.02i$)

| | $C_1$ | $C_2$ | $C_3$ | $C_4$ | $C_5$ | $C_6$ | $C_7$ |
|---|---|---|---|---|---|---|---|
| Equation (11a) | 1.1382 | 0.0636 | 1.3145 | $5.4\ 10^{-6}$ | 8.3323 | −0.5313 | 1.6460 |
| Equation (11b) | 2.0121 | 0.0552 | 1.5840 | 0.1033 | 1.8456 | 1.5870 | 0.3931 |

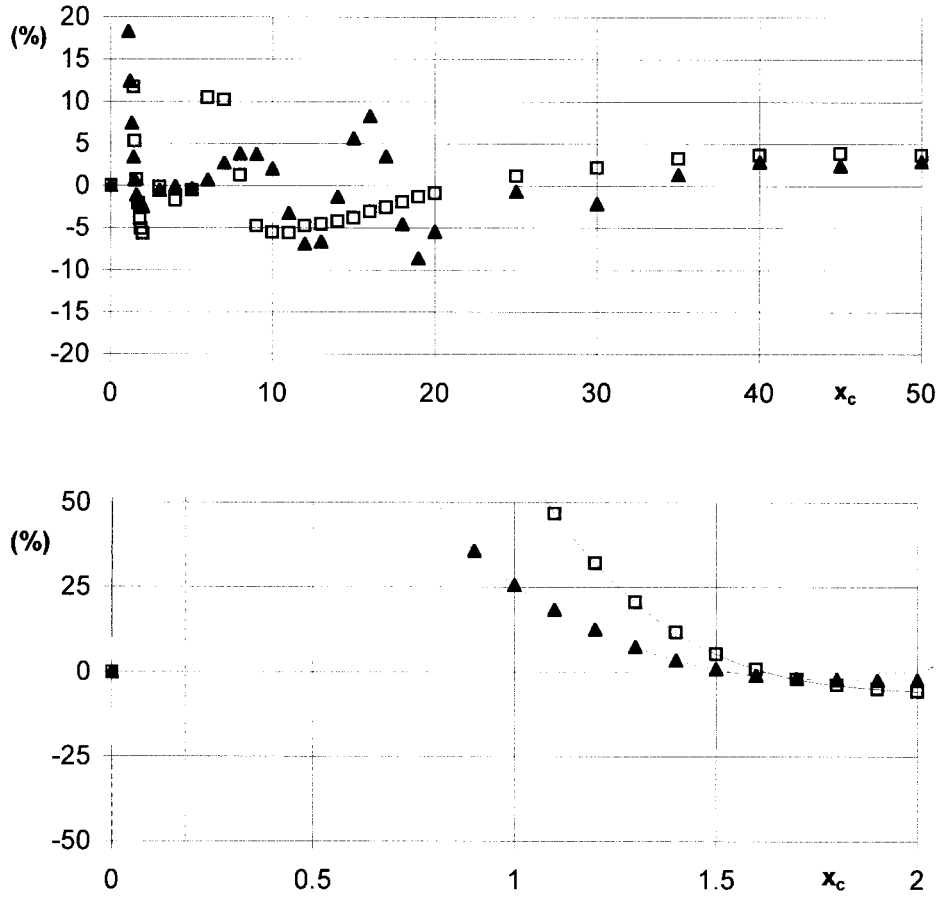


Fig. 5. Error analysis for the comparison of exact and approximate solutions of non-dimensional scattering coefficient for case 2—fly ash ($m = 1.5-0.02i$, $p = 4$, $q = 4$). □, approximation 1; ▲, approximation 2.

of carbon particles. The refractive index used is that proposed by [10] for soot and corroborated by [21] and [23] and the distribution shape parameters ($p = 2$ and $q = 2$) are those proposed by [24]. The extinction coefficient constitutes in this case the object of analysis.

Non-dimensional extinction factors for this case, both for approximations 1 and 2, are compared against the exact values obtained from the Mie theory in Fig. 7. For this complex refractive index, with a significant imaginary part, the function $F(x, m)$ becomes smoother, that is, the characteristic resonance peaks vanish. Due to this fact, and as it can be observed from Fig. 8, that shows the error relative to the exact solution of approximations 1 and 2, both approximations are very good. Moreover, the agreement for approximation 1 is perfect—0% of relative error—for values of $x_c$ greater than 3.0. For $x_c$ values below 3.0 the agreement is still very good—never exceeding 3% of the relative error. Hence, approximation 1 is highly recommendable to be used.

As in the previous cases, approximation 1 for this case requires a computational time 86 times lower than that of the exact solution.

Table 3
Curve fitting constants for non-dimensional extinction coefficient ($m = 2.2-1.12i$)

| | $C_1$ | $C_2$ | $C_3$ | $C_4$ | $C_5$ | $C_6$ | $C_7$ |
|---|---|---|---|---|---|---|---|
| Equation (11a) | 2.8195 | 1.1409 | 0.6865 | 2.6987 | 5.9627 | −2.9669 | 0.67055 |
| Equation (11b) | 1.5809 | 0.3294 | 0.8782 | 6.2145 | 3.9506 | 0 | 0 |

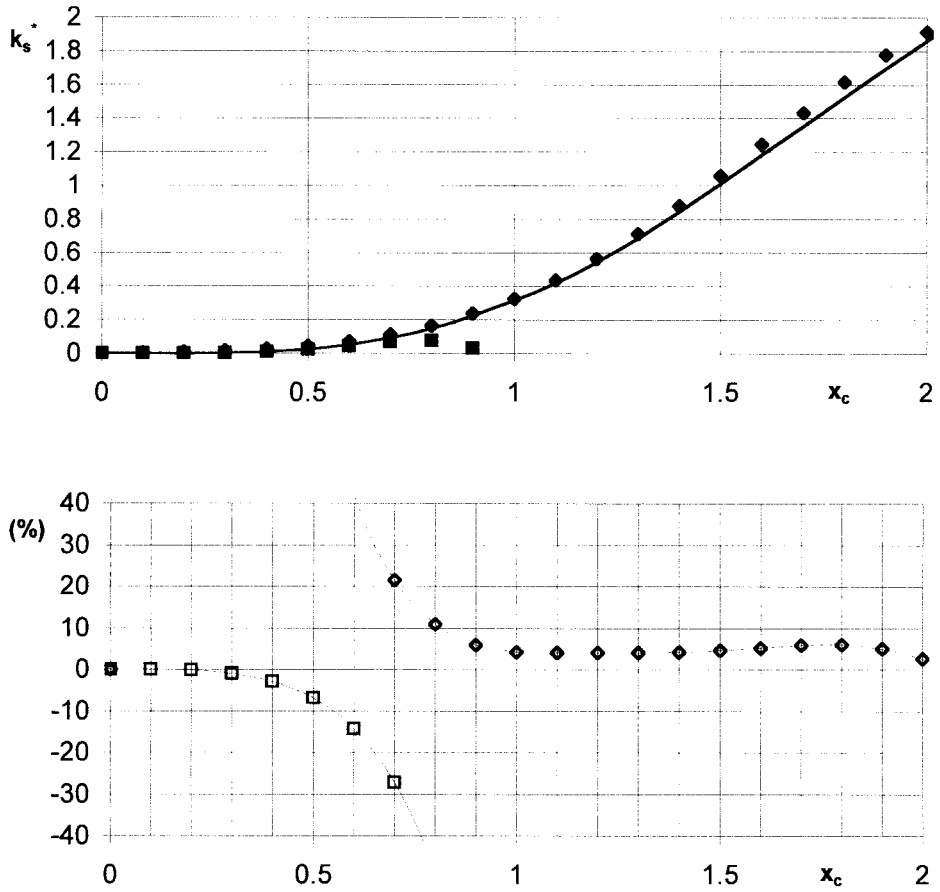


Fig. 6. Comparison and error analysis of exact and approximate solutions of non-dimensional scattering coefficient for case 2—fly ash ($m = 1.5–0.02i$, $p = 4$, $q = 4$). —, exact solution; ■, approximation 3; ◆, approximation 4; □, error of approximation 3; ◇, error of approximation 4.

The values of the constants appearing in Eqs. (11a) and (11b) obtained for this case are depicted in Table 3.

A better insight of the computational time savings that can be achieved through the use of the presently proposed method can be obtained through the observation of Table 4, which summarises those savings.

Table 4
Computational time savings of approximations 1 and 2 when compared to Mie theory

| Reduction in time | Approximation 1 | Approximation 2 |
|---|---|---|
| Case 1 | 320 | 256 |
| Case 2 | 66 | 53 |
| Case 3 | 86 | 69 |
| Average | 157 | 126 |

## 4. Conclusions

There is presently a generalized and legitimate concern in the scientific community with the computational time required for radiative properties calculations for polydispersions, when radiation is to be coupled with CFD computations in the prediction of industrial flames, as both are by themselves very computer time demanding. Therefore, there is an absolute need not to overload the whole simulation with another highly time demanding calculation, which explains the necessity of an extremely efficient algorithm for the calculation of the extinction and scattering coefficients.

In the present work accurate and economic approximations to the Mie theory for the calculation of the extinction and scattering coefficients, based on curve fitting, were proposed. For the sake of accuracy, the characteristic size parameter $x_c$ domain was partitioned into different zones, a different approach being used in

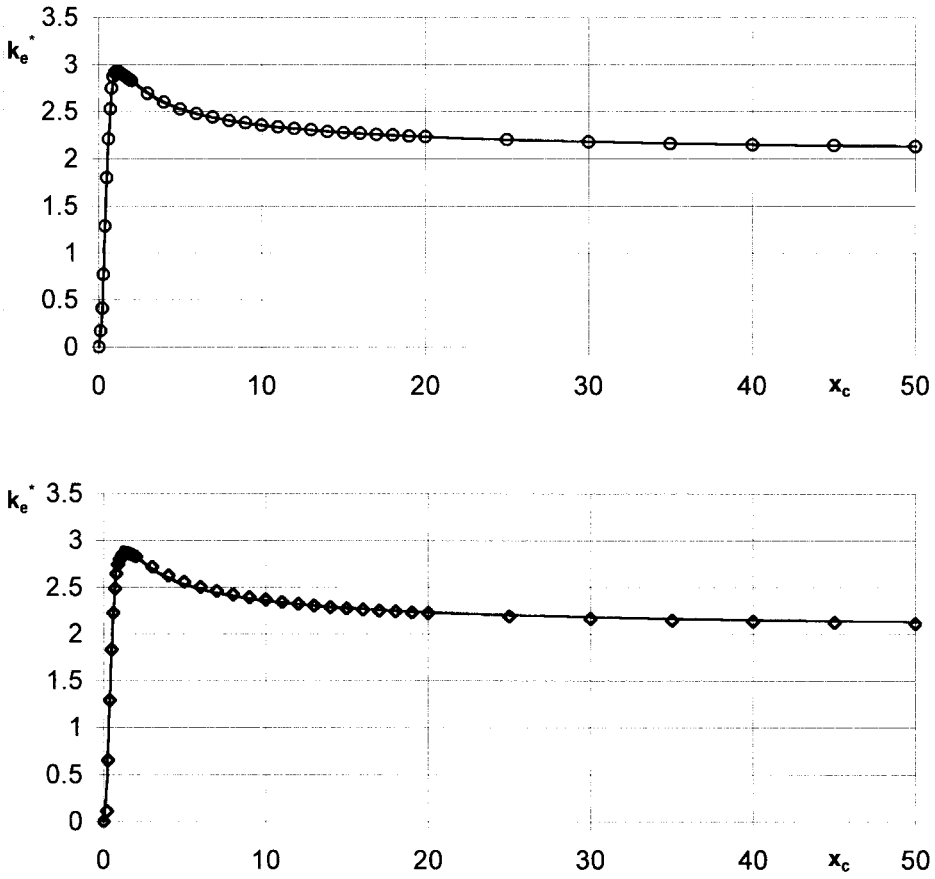


Fig. 7. Comparison of exact and approximate solutions of non-dimensional extinction coefficient for case 3—soot ($m = 2.2-1.12i$, $p = 2$, $q = 2$). —, exact solution; ○, approximation 1; ◇, approximation 2.

each zone. The proposed curve fitting complied with the asymptotic limits of the extinction/scattering coefficients for an isolated particle, besides being more accurate than any other curve fitting approximation known by the authors. The accuracy of the curve fitting approach was largely improved with the present formulation for all values of the size parameter through the use of novel equations which cover a part of the $x_c$ domain where other approximations depart from the Mie theory.

The precision attained through this procedure was for almost all the $x_c$ domain below 5%. However, for isolated circumstances of fly ash and a value of $x_c$ around 0.7 the error can be as much as 28%.

The models proposed herein showed some sensitivity to the shape of the disperse solid phase size distribution, being less accurate (28% relative error) when the distribution was narrower.

When comparing the two proposed curve fitting functional forms (approximations 1 and 2), it was clear that it is not compulsory to model the resonance peaks through a cosine function, since the additional computational effort demanded by the use of that function is not compensated in accuracy, some times being even penalised.

The accuracy achieved and the enormous amount of CPU time saved, that depending on the particle size distribution shape can go up to three-hundredfold when compared with the use of Mie theory, largely justifies the incorporation of the present models in predictive tools to be applied to combustion equipment design and performance.

## Acknowledgement

This work has been partially performed with the financial support of the European Collaborative Research JOULE Programme, under the contract JOF3-CT95-0010.

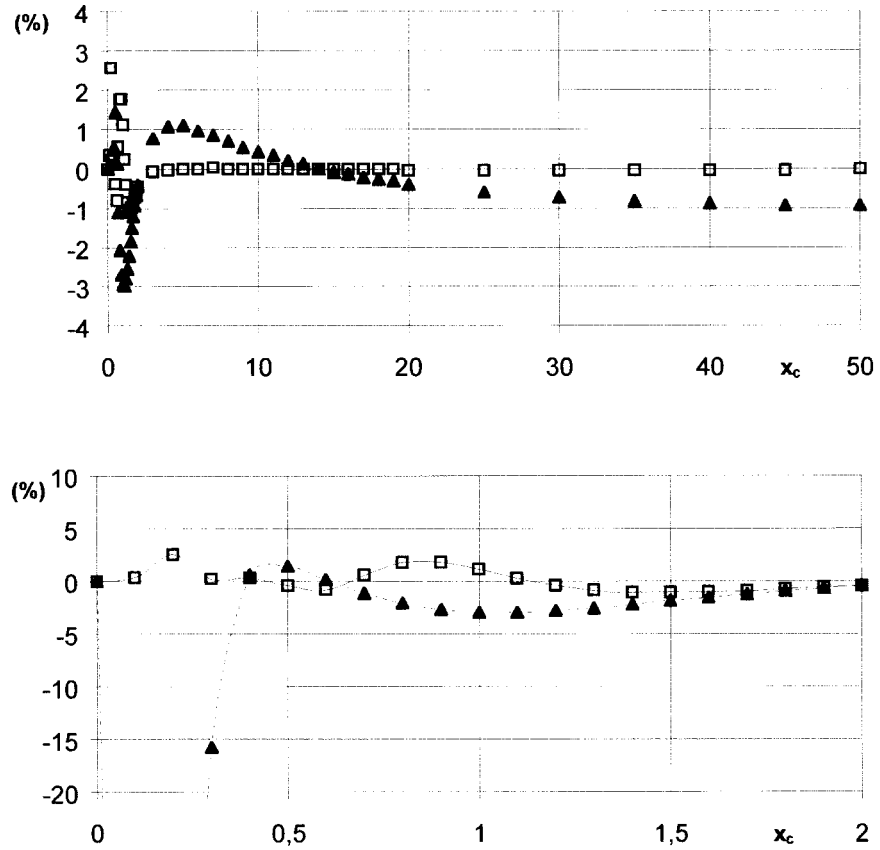


Fig. 8. Error analysis for the comparison of exact and approximate solutions of non-dimensional extinction coefficient for case 3—soot ($m = 2.2-1.12i$, $p = 2$, $q = 2$). □, approximation 1; ▲, approximation 2.

## References


[1] R. Viskanta, M.P. Menguç, Prog. Energy Combust. Sci. 13 (1987) 97–160.

[2] H.C. Hottel, A.F. Sarofim, Radiative Transfer, McGraw-Hill, New York, 1967.

[3] J.R. Howell, in: J.P. Hartnett, T.F. Irvine (Eds.), Advances in Heat Transfer, Vol. 5, Academic Press, New York, 1968.

[4] A.C. Ratzel III, J.R. Howell, ASME J. Heat Transfer 105 (1983) 333–340.

[5] M.P. Menguç, R. Viskanta, ASME J. Heat Transfer 108 (1986) 271–276.

[6] M.P. Menguç, R. Viskanta, J. Quant. Spectrosc. Radiat. Transfer 33 (1985) 533–549.

[7] S. Chandrasekhar, Radiative Transfer, Dover Publications, New York, 1960.

[8] Lockwood FC, Shah NG. Eighteenth Symposium (International) on Combustion, The Combustion Institute, Pittsburgh, 1981. p. 1405–1414.

[9] W.A. Fiveland, ASME J. Heat Transfer 106 (1984) 699–706.

[10] Fiveland WA, Oberjohn WJ, Cornelius DK. COMO: A Numerical Model for Predicting Furnace Performance in Axisymmetric Geometries—Vol. 1, Babcok and Wilcox Company, Report No. DOE/PC/40265-9 (1985).

[11] W.A. Fiveland, J. Thermophysics Heat Transfer 2 (1988) 9–18.

[12] M.G. Carvalho, T. Farias, P. Fontes, in: W.A. Fiveland, A.C. Crosbie, A.M. Smith, T.F. Smith (Eds.), ASME FED—Fundamentals of Radiation Heat Transfer, Vol. 160, 1991.

[13] P.J. Coelho, M.G. Carvalho, ASME J. Heat Transfer 119 (1997) 118–128.

[14] J. Yuan, V. Semião, M.G. Carvalho, J. Inst. Energy LXX (1997) 57–70.

[15] H.C. Van de Hulst, Light Scattering by Small Particles, Wiley, New York, 1957.

[16] N. Lallement, R. Weber, Int. J. Heat Mass Transfer 39 (1996) 3273–3286.

[17] Y.U. Khan, D.A. Lawson, R.J. Tucker, Int. J. Heat Mass Transfer 40 (1997) 3581–3593.

[18] P.S. Cumber, M. Fairweather, H.S. Ledin, Int. J. Heat Mass Transfer 41 (1998) 1573–1584.

[19] O. Marin, R.O. Buckius, Int. J. Heat Mass Transfer 41 (1998) 2877–2892.

[20] O. Marin, R.O. Buckius, Int. J. Heat Mass Transfer 41 (1998) 3881–3897.
[21] M.F. Modest, Radiative Heat Transfer, McGraw-Hill, New York, 1993.
[22] M.A. Al-Nimr, V.S. Arpaci, ASME J. Heat Transfer 114 (1992) 950–957.
[23] M.P. Menguç, R. Viskanta, Combust. Sci. Technol. 44 (1985) 143–159.
[24] A.G. Blokh, Heat Transfer in Steam Boiler Furnaces, Hemisphere, Washington, DC, 1988.
[25] R.B. Penndorf, J. Optical Soc. America 52 (1962) 896–904.
[26] S. Bard, P.J. Pagni, ASME J. Heat Transfer 103 (1981) 357–362.
[27] X. Li, R. Tankin, Combust. Sci. Technol. 56 (1987) 65–76.
[28] V. Semião, P. Andrade, M.G. Carvalho, Fuel 75 (1996) 1707–1714.
[29] A.H. Stroud, D. Secrest, Gaussian Quadrature Formulas, Prentice-Hall, London, 1966.